

Navigation by anomalous random walks on complex networks

Tongfeng Weng^{1,*}, Jie Zhang², Moein Khajehnejad¹, Michael Small^{3,4}, Rui Zheng¹, and Pan Hui^{1,+}

¹HKUST-DT System and Media Laboratory, Hong Kong University of Science and Technology, HongKong

²Centre for Computational Systems Biology, Fudan University, China

³The University of Western Australia, Crawley, WA 6009, Australia

⁴Mineral Resources Flagship, CSIRO, Kensington, WA, Australia

*wtongfeng2006@163.com

+panhui@cse.ust.hk

ABSTRACT

Anomalous random walks having long-range jumps are a critical branch of dynamical processes on networks, which can model a number of search and transport processes. However, traditional measurements based on mean first passage time are not useful as they fail to characterize the cost associated with each jump. Here we introduce a new concept of mean first traverse distance (MFTD) to characterize anomalous random walks that represents the expected traverse distance taken by walkers searching from source node to target node, and we provide a procedure for calculating the MFTD between two nodes. We use Lévy walks on networks as an example, and demonstrate that the proposed approach can unravel the interplay between diffusion dynamics of Lévy walks and the underlying network structure. Interestingly, applying our framework to the famous PageRank search, we can explain why its damping factor empirically chosen to be around 0.85. The framework for analyzing anomalous random walks on complex networks offers a new useful paradigm to understand the dynamics of anomalous diffusion processes, and provides a unified scheme to characterize search and transport processes on networks.

Introduction

Complex networks are ubiquitous in the real world ranging from sociology to biology and technology¹. Going beyond the interesting topological properties, quantifying the impact of structural organization of networks on transport processes has become one of the most important topics. As a paradigmatic transport process, random walks on complex networks have been intensively studied²⁻⁶. A variety of measurements including mean first passage time (MFPT)², first passage time⁴, and average trapping time⁶ have been proposed, providing a comprehensive characterization of random walks on networks. Moreover, these studies also facilitate our understanding of diverse dynamical processes on networks including epidemic spreading⁷, synchronization⁸, and transportation⁹.

However, for random walks, the walker is confined only to the neighbourhood of a node in each jump, which cannot model some real situations¹⁰, and also impedes search and transport efficiency on networks⁴. This limitation is circumvented by the model of Lévy walks in natural condition^{11,12}. Recently, intensive attention has been devoted to anomalous random walks on networks, such as Lévy walks^{13,14}, traditional web surfing¹⁵, and even electric signals transmitted in brain networks¹⁰. One striking feature of anomalous random walks is having the long-range hopping (i.e., the walker can hop to far away nodes not directly connected to its current position). In fact, the occurrence of long-range hopping is frequently encountered in our life. For example, we usually communicate with people socially close to us, but also occasionally with those that are unconnected¹⁴. Analogously, when doing web surfing, one usually proceeds by following the hyperlinks but casually may open a new tab to look for the related topic¹⁰. Although it is widely agreed that anomalous random walks represent an important branch of search and transport processes on networks, how to characterize anomalous random walks and specifically, to uncover the interplay between their dynamics and the underlying network structure has not been addressed. Traditional measurements like the mean first passage time neglect the difference between the cost associated with the nearest-neighbor jump and the long-range hopping, therefore cannot properly characterize anomalous random walks on networks.

In this paper, we propose the mean first traverse distance that represents the expected traverse distance required by a walker moving from a source node to a target node. Importantly, this allows the cost associated with the hopping to be taken into account in the characterization of anomalous random walks; this therefore overcomes the problems of traditional measurements adopted in general random walks. We obtain analytically the MFTD and the global MFTD on arbitrary networks. Results on Lévy walks demonstrate that these measurements can effectively characterize the relationship between network structure

and anomalous random walks. Interestingly, when applied to the PageRank search, we demonstrate that the optimal damping factor occurs at around 0.85 in real web networks which is consistent with our empirical finding. The new metric enables effective characterization of dynamics of anomalous random walks on networks, which promises more efficient search and transport processes on networks.

Results

The MFTD of anomalous random walks We start from an undirected network consisting of N nodes. The connectivity of nodes is fully described by a symmetric adjacency matrix A , whose entry $a_{ij} = 1$ (0) if nodes i and j are (not) connected. For anomalous random walks, at each time step, the walker jumps from current node i to node j with a nonzero transition probability p_{ij} regardless of the connection profile of node i . Take Lévy walks on networks for example, the transition probability is defined as $p_{ij} = d_{ij}^{-\alpha} / \sum_k d_{ik}^{-\alpha}$, where α is the tuning exponent lying in the interval $0 \leq \alpha < \infty$ and d_{ij} is the shortest path length between nodes i and j ¹³. To characterize anomalous random walks, we propose a concept of the MFTD l_{ij} , which is the expected distance taken by a walker to first reach node j starting from node i . Intuitively, the traverse distance in one-step jump is shorter for a walker when nodes are directly connected, while this distance tends to be larger for indirectly linked nodes. Inspired by the empirical findings that the lengths of links usually obey a power law distribution¹⁶, we adopt the power function $c_{ij} = d_{ij}^\beta$ to describe the effective distance of one-step jump, where β named the cost exponent is a nonnegative value. In this situation, if the first step of the walk is to node j , the expected traverse distance required is d_{ij}^β ; if it is to some other node k , the expected traverse distance becomes l_{kj} plus d_{ik}^β for the previous step already taken. Thus, we have

$$l_{ij} = p_{ij}d_{ij}^\beta + \sum_{k \neq j} p_{ik}(l_{kj} + d_{ik}^\beta). \quad (1)$$

Using the Markov chains theory^{17,18}, the MFTD l_{ij} of a anomalous random walk (see appendices) becomes

$$l_{ij} = T_{ij} \sum_k \left(\sum_m p_{km} d_{km}^\beta \right) w_k + \sum_k (z_{ik} - z_{jk}) \left(\sum_m p_{km} d_{km}^\beta \right), \quad (2)$$

where w_k is the k th component of the stationary distribution of the anomalous random walk, T_{ij} is the MFPT from node i to node j , and z_{ij} is an element of the fundamental matrix $Z = (I - P + W)^{-1}$. Specifically, when $\beta = 0$, the effective distances of one-step jump are same (i.e., $c_{ij} = 1$). In this situation, it is easy to verify that the MFTD l_{ij} reduces to the MFPT T_{ij} , which means that our paradigm can incorporate the commonly used MFPT as a special case. To further evaluate the search efficiency of an anomalous walker, we calculate the global MFTD $\langle L \rangle$ by averaging Eq. (2) over all pairs of source and target nodes, that is,

$$\langle L \rangle = \frac{1}{N(N-1)} \sum_i \sum_j l_{ij}. \quad (3)$$

Plugging Eq. (2) into Eq. (3), we have

$$\langle L \rangle = \langle T \rangle \sum_i \left(\sum_j p_{ij} d_{ij}^\beta \right) w_i, \quad (4)$$

where $\langle T \rangle$ is the average of MFPTs over all pairs of nodes in the networks (see appendices). Here, $\langle L \rangle$ quantifies the ability of the anomalous walker to search and transport at the global scale on the network. In this context, smaller $\langle L \rangle$ represents a more effective way of achieving mobility. In the following we will demonstrate how these measurements can effectively characterize diverse anomalous random walks on networks.

The MFTD scheme for characterizing Lévy walks We first address a specific anomalous random walk — Lévy walks on networks. A Lévy walk exerts a power-law transition probability with the distance given by $p_{ij} = d_{ij}^{-\alpha} / \sum_k d_{ik}^{-\alpha}$. Clearly, the tuning exponent α plays an important role in controlling the trade off between short-range and long-range jumping in one step, which in turn fully determines the behaviors of the Lévy walk. Specially, when α is very small, the walker visits all nodes with approximately equivalent probability. In contrast, the walker possibly only hop to the nearest neighbors at an extremely large α . In this context, the Lévy walk degenerates to the generic random walk². Using the balance condition, the stationary distribution of the Lévy walk can be expressed as

$$w_i = \frac{\sum_k d_{ik}^{-\alpha}}{\sum_i \sum_j d_{ij}^{-\alpha}}. \quad (5)$$

Inserting the above equation and the transition probability into Eq. (2) yields

$$l_{ij} = \frac{z_{jj} - z_{ij}}{\sum_m d_{jm}^{-\alpha}} \sum_i \sum_j d_{ij}^{\beta-\alpha} + \sum_k (z_{ik} - z_{jk}) \frac{\sum_m d_{km}^{\beta-\alpha}}{\sum_m d_{km}^{-\alpha}}. \quad (6)$$

Similar calculation applied to Eq. (4), the global MFTD $\langle L \rangle$ of Lévy walks reads

$$\langle L \rangle = \langle T \rangle \frac{\sum_i \sum_j d_{ij}^{\beta-\alpha}}{\sum_i \sum_j d_{ij}^{-\alpha}}. \quad (7)$$

To test the validity of Eq. (7), we report both the numerical and theoretical results of the global MFTD for Lévy walks taking place in planar Sierpiński gasket¹⁹ and the (1,2)-flower model²⁰. These two networks are typical hierarchical nets having the same number of nodes and edges but exhibiting apparently distinct structure organizations, which can favor us to explore how the network structure influences the behavior of a Lévy walk directly. To achieve the numerical results, we compute the traverse distance required for a walker to travel from a source node to a target node chosen randomly and average over the ensemble of 50,000 independent runs for each test. Fig. 1 shows an excellent agreement between numerics and Eq. (7) for the different cost exponents β . In particular, when $\beta = 0$, the minimum of $\langle L \rangle$ occurs at $\alpha = 0$ regardless of the network structures, which reproduces the previous results based on the MFPT²¹. However, this result is unreasonable in practice without considering the distinct costs induced by the nearest-neighborhood jumps and the long-range hops. In contrast, we find that when $\beta > 0$, the profiles of different network organizations show clearly distinct behaviors. Specially, the profiles of the planar Sierpiński gasket display a clear minimum in the medium range α , which minimizes the search distance, (i.e., the global mean first traverse distance). However, such behavior is absent for the (1,2)-flower model for $\beta > 0$, where they present a clearly monotonous tendency, see Fig. 1 (b). Such difference can be intuitively explained when referring to their topological properties. Specially, the Sierpiński gasket is a fractal network without the “small-world” property¹⁹, see its topological structure in Fig. 1 (a). In contrast, the (1,2)-flower network has the “small-world” feature and the “scale-free” characteristics²⁰, as shown in Fig. 1 (b). Meanwhile, we also notice that, when α is large, the transition probability of the Lévy walk degenerates to a generic random walk. Thereby, all curves approach a fixed value for $\alpha > 9$, see in Fig. 1 (a) and (b), as expected.

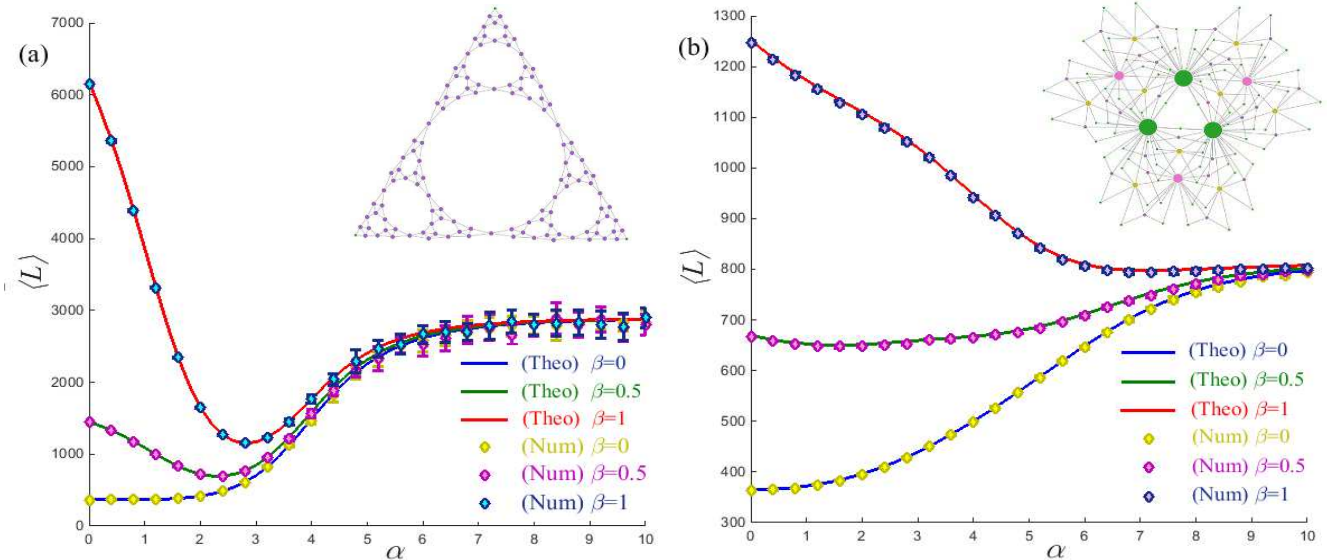


Figure 1. The global MFTD $\langle L \rangle$ as a function of α , for Lévy walks on (a) the planar Sierpiński gasket and (b) the (1,2) flower model with the same size $N = 366$ nodes and $\beta = 0, 0.5, 1$, respectively. Symbols represent the values of $\langle L \rangle$ found numerically, while solid lines correspond to the theoretical prediction of Eq. (7). Error bars represent the mean first traverse distance $\langle L \rangle$ over 20 tests and each test is averaged over the ensemble of 50,000 independent runs.

To further demonstrate the difference induced by network structure, we observe the size effect on the global MFTD $\langle L \rangle$ of the planar Sierpiński gasket and the (1,2)-flower model. We find that the profiles of each network present the same tendency for different network sizes N , see Fig. 2 (a) and (b). Interestingly, the result presented in Fig. 2 (a) clearly shows the presence

of a minimum $\langle L \rangle$ for different network sizes at the same exponent $\alpha = 2.8$. The way in which $\langle L \rangle$ scales with network size N on the planar Sierpiński gasket seems to follow rather different behaviors depending on the tuning exponent α . Specially, when $\alpha \neq 2.8$, the global MFTD $\langle L \rangle$ follows a power law with network size N , see in Fig. 2 (c). It is supported by observing the almost invariant values of the successive slopes δ_s obtained from $\ln \langle L \rangle$ versus $\ln N$, as shown in the inset of Fig. 2 (c). Conversely, for $\alpha = 2.8$, the successive slopes δ_s present a clearly decreasing tendency. However, for the (1,2)-flower model, the $\langle L \rangle$ follows approximately a power law with network size N , see in Fig. 2 (d). Note that here we choose the cost exponent $\beta = 1$ for convenience. However, such behavior of $\langle L \rangle$ versus N is general for an arbitrary cost exponent β .

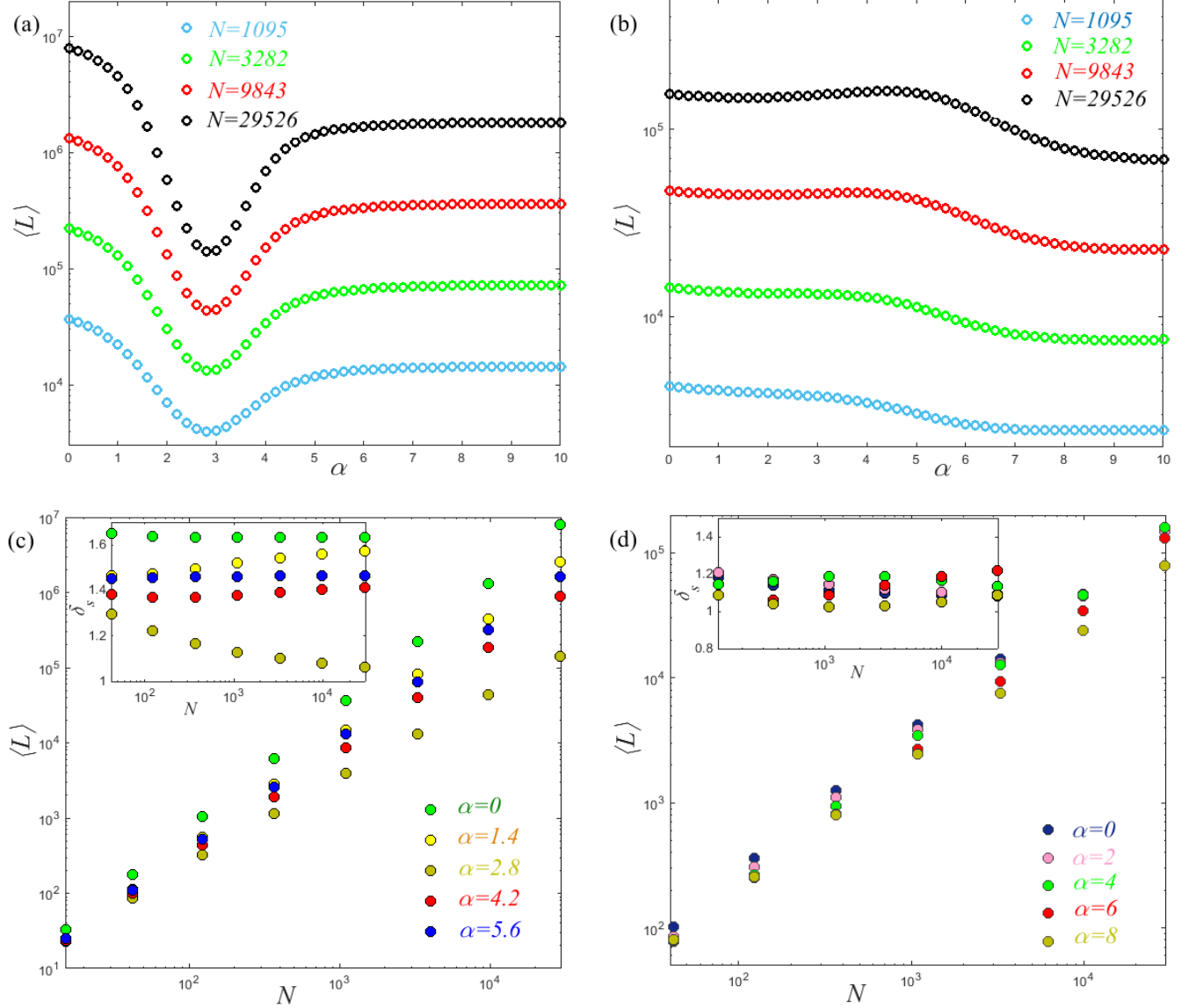


Figure 2. The global MFTD $\langle L \rangle$ as a function of α for Lévy walks on (a) the planar Sierpiński gasket and (b) the (1,2) flower model over different network sizes N . The behaviors of $\langle L \rangle$ versus N for different exponents α on the planar Sierpiński gasket (c) and the (1,2) flower model (d). In the insets, we show the plots of the successive slopes δ_s obtained from $\ln \langle L \rangle$ versus $\ln N$. Note that here we set the cost exponent $\beta = 1$.

Clearly, from Eq. (7), the cost exponent β plays an important role in controlling the search efficiency for Lévy walks. In order to explore how the optimal search efficiency of a Lévy walk changes with respect to the cost exponent β , we investigate the interplay between β and α for various networks including three synthetic models (the Barabási-Albert (BA) model²², the planar Sierpiński gasket¹⁹, and the (u,v)-flower model²⁰) and two real networks (the “Dolphin” network²³ and an e-mail network²⁴). Here, for a fair comparison, we calculate the measurement $\log_N \langle L \rangle$ in the (α, β) plane for eliminating the size effect of networks. Generally, regions with smaller $\log_N \langle L \rangle$ indicate an efficient way of search and transport based on Lévy

walks. Fig. 3 shows contour maps of $\log_N \langle L \rangle$ in the (α, β) plane computed for these selected networks. Interestingly, we find that distinct network structures lead to different patterns in the corresponding (α, β) plane. Specifically, the (α, β) planes generated from networks having the “small-world” characteristics, such as the BA model and the (1,2)-flower model, demonstrate an “estuary” pattern, implying that Lévy walks are not the optimal way to search when $\beta > 0.4$. In contrast, typical fractal networks without the “small-world” property, for example, the planar Sierpiński gasket and the (4,5)-flower model, result in a striking “flame” in the (α, β) planes, suggesting that there exists an optimal tuning exponent α , which minimizes the traverse distance for a broad range of cost exponents β . However, none of these patterns match the ones found in the Dolphin network and the e-mail network, whose (α, β) planes show “rippled” features, meaning that the optimal exponent α gradually increases with the cost exponent β . The (α, β) plane uncovers the relationship between network structure and the behavior of Lévy walks, which provides information to help designing more effective search strategies and transport mechanisms in different environments.

Furthermore, we follow the spirit of the MFPT, and extract more statistics from the MFTD. Here, we introduce the average trapping distance (ATD) defined as follows:

$$L_j = \frac{1}{1 - w_j} \sum_{m=1}^N w_m l_{mj}. \quad (8)$$

The ATD L_j quantifies the mean of MFTD l_{mj} to the trap node j , taken over all starting points with the stationary distribution. Submitting the results of Eqs. (5) and (6) into Eq. (8) yields (see appendices)

$$L_j \approx \frac{z_{jj}}{K_j} \sum_i \sum_j d_{ij}^{\beta - \alpha}, \quad (9)$$

where $K_j = \sum_m d_{jm}^{-\alpha}$ named the long-range degree of node j ¹³. Specifically, when α is small, the diagonal values of Z are almost same. In this context, a clear scaling behavior emerges such that $L_j \sim K_j^{-1}$ regardless of the underlying network structure. This is supported by observing the plots of $\ln L_j$ vs $\ln K_j$ shown in Fig. 4 (a) and (b). With an increase of α , the slope of $\ln L_j$ versus $\ln K_j$ gradually decreases and finally asymptotically approaches to that of random walks as described in Ref. 4. Results demonstrate the important role of α in shaping the ATD. Meanwhile, from Eq. (9), it is easy to verify that the relationship between $\ln L_j$ and $\ln K_j$ does not depend on the cost exponent β . So, the profiles present a similar tendency for different cost exponents β as illustrated in Fig. 4 (c) and (d). We further find a linear relationship between $\ln L_j$ and β , when fixing the tapping position j and the tuning exponent α , see the insets in Fig. 4 (c) and (d). The results are consistent with our theoretical prediction of the relationship $\ln L_j \sim C\beta$, where C is a constant value related to the fractal dimension of a given network (see appendices).

The optimal condition of the PageRank search based on the MFTD theory We finally apply the MFTD theory to characterize the famous PageRank search¹⁵. The PageRank search is widely used to compute the relevance of web pages. The transition probability p_{ij} of the PageRank search is

$$p_{ij} = \mu \frac{a_{ij}}{k_i} + (1 - \mu) \frac{1}{N} \quad (10)$$

where $k_i = \sum_l a_{il}$ is the degree of node i and μ is the damping factor lying in the range $[0, 1]$. We investigate the global MFTD $\langle L \rangle$ for the PageRank search on two real networks (web-Stanford²⁵ and Ego-Facebook²⁶). The results presented in Fig. 5 (a) and (b) indicate the existence of a minimum $\langle L \rangle$ for different cost exponents β at the same value of the damping factor $\mu \approx 0.85$, where optimal search is achieved. This is further supported by observing the contour maps of the (μ, β) plane, where for $\mu \approx 0.85$, the global MFTD $\langle L \rangle$ is near its minimum value for a very broad range of β , see in Fig. 5 (c) and (d). This can explain why the ad hoc damping factor of the PageRank search is suggested to be set around 0.85. Moreover, we notice that the minimum $\langle L \rangle$ of the PageRank search is much smaller than that of generic random walks (i.e., $\mu = 1$), which in some extent demonstrates the advantage of taking the PageRank search instead of generic random walks.

Discussion

In summary, we have introduced the concept of the MFTD, a measure that takes into account of the cost of jumps in anomalous random walks, therefore is particularly suited to capture the interplay between the diffusion dynamics of anomalous random walks and underlying network structures. We obtain an exact expression for the MFTD and the global MFTD of anomalous random walks on complex networks. We show that our paradigm provides a unified scheme to characterize diffusion processes on networks, which incorporates the commonly used MFPT as a special case.

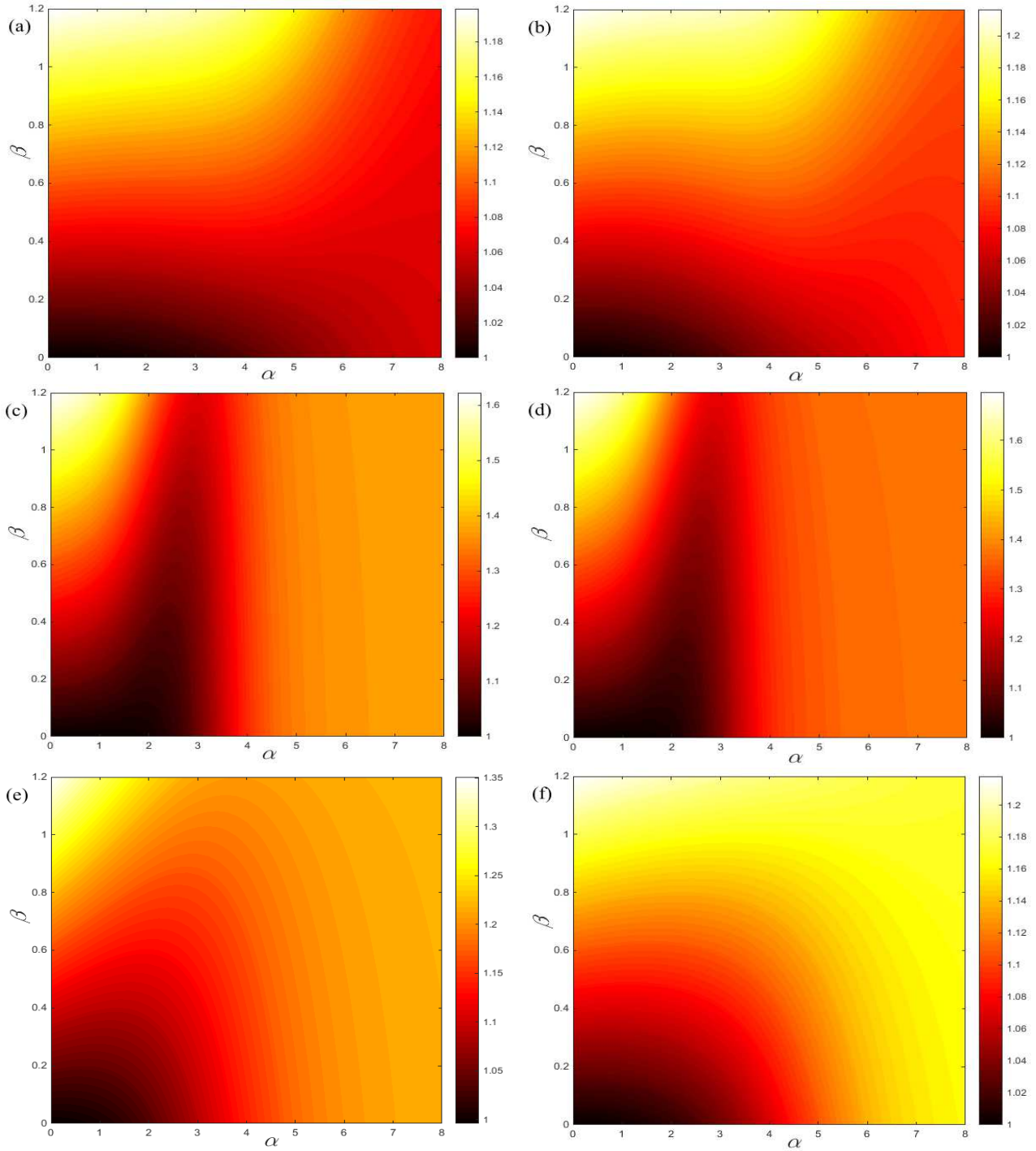


Figure 3. The measurement $\log_N \langle L \rangle$ in the (α, β) parameter plane of (a) the BA model, (b) the (1,2)-flower model, (c) planar Sierpiński gasket, (d) the (4,5)-flower model, (e) the “Dolphin” network²³, and (f) the e-mail network²⁴.

We then demonstrate the effectiveness of these measures by applying them to Lévy walks. We find that distinct network structures result in different patterns in the (α, β) planes, which explores the effect of the cost exponent β on behaviors of Lévy walks with respect to network structure. Moreover, when addressing the trapping problem of Lévy walks, we find that its behavior only depends on the tuning exponent α irrespective of the cost exponent β . In particular, when α is smaller, it presents a uniformly scaling feature regardless of network structure. These findings enrich our understanding of interplay between dynamics of Lévy walks and network structure. To implement Lévy walks, we need to compute all shortest paths of

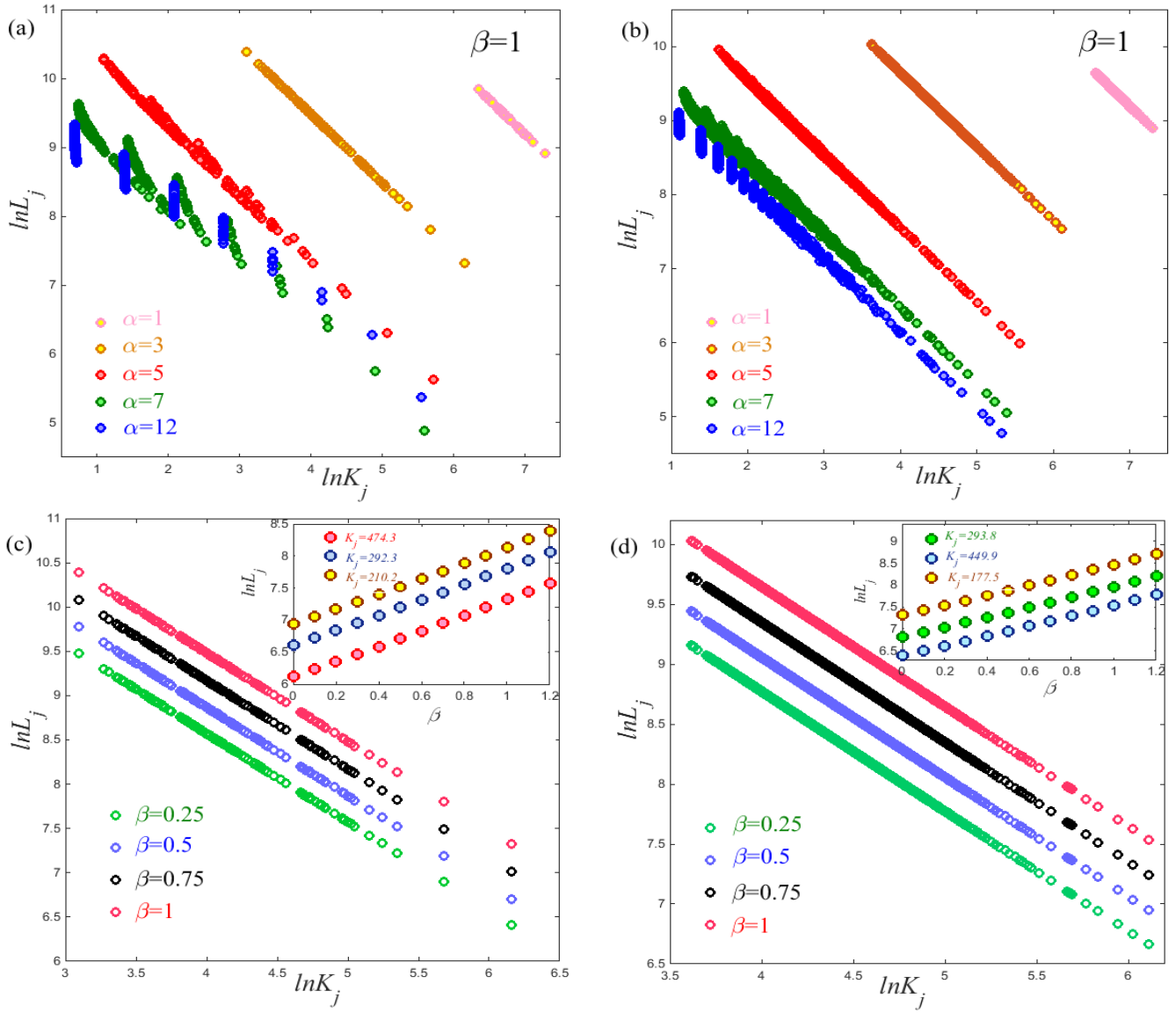


Figure 4. Plots of $\ln L_j$ versus $\ln K_j$ are presented for (a) the (1,2)-flower model and (b) the BA model with network size $N = 3282$. The same plots with respect to different cost exponents β for (c) the (1,2)-flower mode and (d) the BA model under the cost exponent $\alpha = 3$. In the inset, we show $\ln L_j$ versus β for different trapping nodes j . Note that here the values of $\ln L_j$ are calculated based on the Eq. (8).

a network which involves high computational costs for large networks. In practice, one can use several excellent algorithms such as the preprocessing algorithm²⁸, which is one of possible solution for this problem. Nonetheless, the results show that for a broad range of the cost exponent β , the global MFTD $\langle L \rangle$ of Lévy walks is much smaller than that of generic random walks, which demonstrates the efficient for search and transport based on Lévy walks.

Finally, application to the famous PageRank search shows that the empirical damping factor is optimal at 0.85 for the cost exponent lying in the range $[0.9, 1.3]$, at which individuals can optimize search in traverse distance. It is suggested that the time required for opening a new tab is approximately equivalent to that of following the hyperlinks for several turns for a related topic search. Thereby, in practice, the damping factor of the PageRank search is chosen around 0.85. Overall, our findings offer a new framework to understand the diffusion dynamics of anomalous random walks on complex networks.

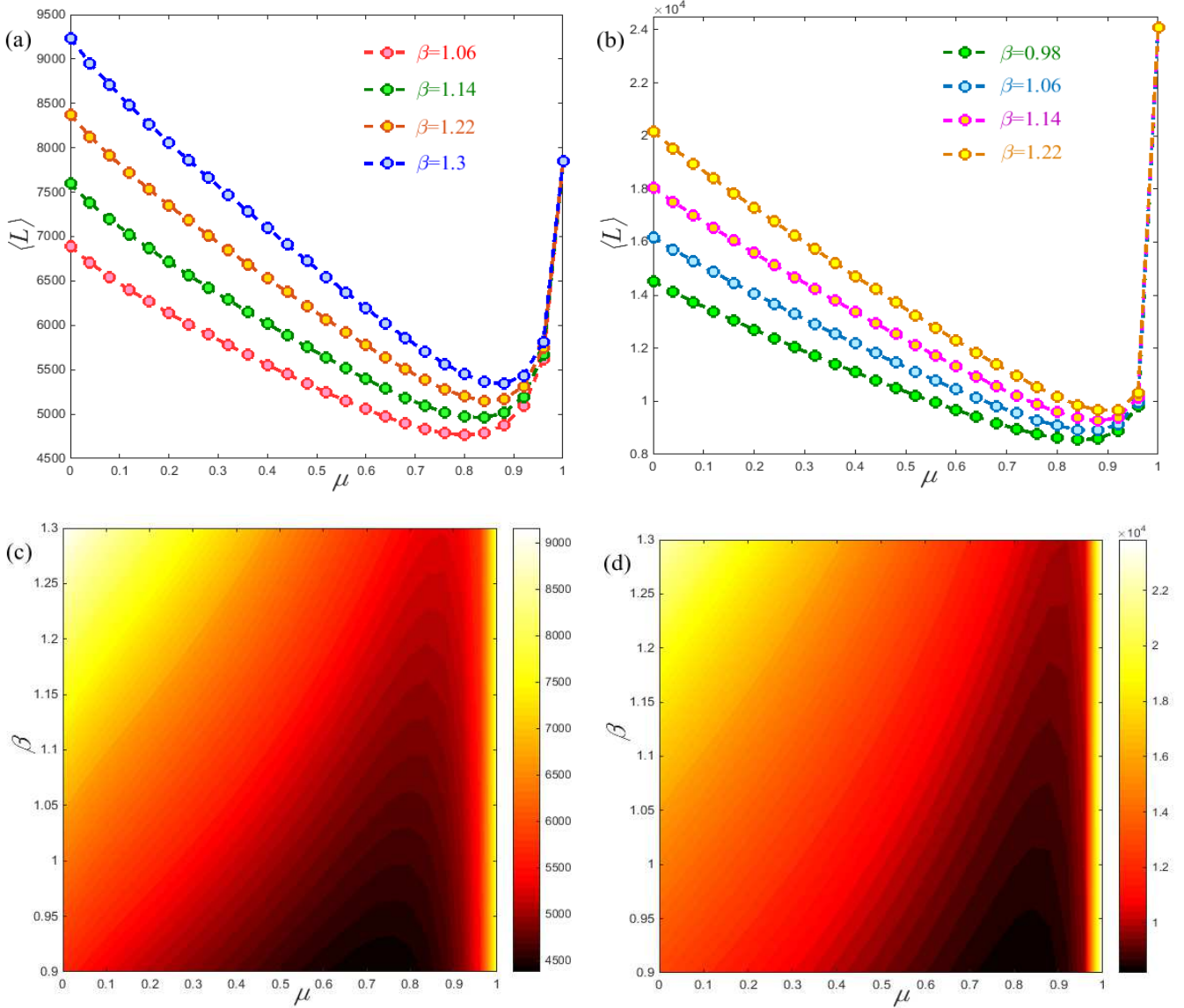


Figure 5. The global MFTD $\langle L \rangle$ as a function of the damping factor μ , for the PageRank search on (a) web-Stanford²⁵ and (b) Ego-Facebook²⁶. Symbols correspond to the theoretical prediction of Eq. (4). The global MFTD $\langle L \rangle$ in the (β, μ) parameter plane of (c) web-Stanford and (d) Ego-Facebook. Note that the web-Stanford network used here is a subgraph extracted from the original one for computation convenience with $N = 2004$.

Appendices

The analytic expression of mean first traverse distance We follow the derivation of MFPT in Ref. 17 to calculate the MFTD on networks. We consider an arbitrary finite network consisting of N nodes. The connectivity is represented by the adjacency matrix A , whose entries $a_{ij} = 1$ (or 0) if there is (not) a link from nodes i to j . Let D denote the distance matrix with elements d_{ij} representing the shortest path length from node i to node j . In the process of anomalous random walks, at each step, the walker starting from node i arrives to node j with a non-zero transition probability p_{ij} regardless of the connectivity between nodes i and j . If the first step of the walk is to node j , the expected traverse distance required is d_{ij}^β ; if it is to some other node k , the expected traverse distance becomes l_{kj} plus d_{ik}^β for the previous step already taken. Thus, we obtain

$$l_{ij} = p_{ij}d_{ij}^\beta + \sum_{k \neq j} p_{ik}(l_{kj} + d_{ik}^\beta), \quad (11)$$

where l_{ij} is the mean first traverse distance from node i to node j . Since $l_{jj} = 0$, Eq. (11) can be rewritten as

$$l_{ij} = \sum_m p_{im} d_{im}^\beta + \sum_k p_{ik} l_{kj}. \quad (12)$$

Let r_i denote the mean first return distance to node i starting from node i . In the same manner, r_i can be represented as

$$r_i = \sum_k p_{ik} (l_{ki} + d_{ik}^\beta). \quad (13)$$

Combining Eq. (12) and Eq. (13) together, we obtain the relation

$$(I - P)L = C - R, \quad (14)$$

where I denotes the identity matrix, and

$$L = \begin{pmatrix} l_{11} & l_{12} & \cdots & l_{1n} \\ l_{21} & l_{22} & \cdots & l_{2n} \\ \vdots & \vdots & \vdots & \vdots \\ l_{n1} & l_{n2} & \cdots & l_{nn} \end{pmatrix}, \quad (15)$$

$$C = \begin{pmatrix} \sum_k p_{1k} d_{1k}^\beta & \sum_k p_{1k} d_{1k}^\beta & \cdots & \sum_k p_{1k} d_{1k}^\beta \\ \sum_k p_{2k} d_{2k}^\beta & \sum_k p_{2k} d_{2k}^\beta & \cdots & \sum_k p_{2k} d_{2k}^\beta \\ \vdots & \vdots & \vdots & \vdots \\ \sum_k p_{Nk} d_{Nk}^\beta & \sum_k p_{Nk} d_{Nk}^\beta & \cdots & \sum_k p_{Nk} d_{Nk}^\beta \end{pmatrix}, \quad (16)$$

$$R = \begin{pmatrix} r_1 & 0 & \cdots & 0 \\ 0 & r_2 & \cdots & 0 \\ \vdots & \vdots & \vdots & \vdots \\ 0 & 0 & \cdots & r_n \end{pmatrix}. \quad (17)$$

Multiplying both sides of Eq. (14) by the matrix $W = \begin{pmatrix} w_1 & w_2 & \cdots & w_N \\ w_1 & w_2 & \cdots & w_N \\ \vdots & \vdots & \vdots & \vdots \\ w_1 & w_2 & \cdots & w_N \end{pmatrix}$ with the element w_i being the i th component

of the stationary distribution, and using the fact that

$$W(I - P) = 0 \quad (18)$$

gives

$$WC - WR = 0. \quad (19)$$

From Eq. (19), the mean first return distance r_i reads

$$r_i = \frac{\sum_k \left(\sum_m p_{km} d_{km}^\beta \right) w_k}{w_i}. \quad (20)$$

Since the matrix $(I - P + W)$ has an inverse¹⁷, we denote $Z = (I - P + W)^{-1}$. Multiplying both sides of Equation (14) by Z and using the fact that

$$I - W = Z(I - P) \quad (21)$$

gives

$$L = ZC - ZR + WL. \quad (22)$$

From the above equation, l_{ij} and l_{jj} can be expressed as

$$l_{ij} = \sum_k z_{ik} \left(\sum_m p_{km} d_{km}^\beta \right) - z_{ij} r_j + (wL)_j \quad (23)$$

and

$$l_{jj} = \sum_k z_{jk} \left(\sum_m p_{km} d_{km}^\beta \right) - z_{jj} r_j + (wL)_j. \quad (24)$$

Since $l_{jj} = 0$ and using Eq. (20), one has

$$l_{ij} = T_{ij} \sum_k \left(\sum_m p_{km} d_{km}^\beta \right) w_k + \sum_k (z_{ik} - z_{jk}) \left(\sum_m p_{km} d_{km}^\beta \right), \quad (25)$$

where $T_{ij} = \frac{z_{jj} - z_{ij}}{w_j}$ is the mean first passage time.

The analytic expression of global mean first traverse distance To further evaluate the search efficiency based on anomalous random walks, we introduce the global mean first traverse distance defined as

$$\langle L \rangle = \frac{1}{N(N-1)} \sum_i \sum_j l_{ij}. \quad (26)$$

Plugging Eq. (25) into Eq. (26), we obtain

$$\langle L \rangle = \langle T \rangle \sum_k \left(\sum_m p_{km} d_{km}^\beta \right) w_k + \frac{1}{N(N-1)} \sum_i \sum_j \sum_k (z_{ik} - z_{jk}) \left(\sum_m p_{km} d_{km}^\beta \right), \quad (27)$$

where $\langle T \rangle = \frac{1}{N(N-1)} \sum_i \sum_j T_{ij}$ is the global mean first passage time. Since column vectors of the matrix C are the same, the column vectors of the matrix ZC is also the same. Then, the last term of Eq. (27) will vanish due to that

$$\sum \sum (ZC - (ZC)^T) = 0, \quad (28)$$

where the matrix $(ZC)^T$ represents the transpose of matrix ZC . So, the expression for $\langle L \rangle$ is reduced to

$$\langle L \rangle = \langle T \rangle \sum_k \left(\sum_m p_{km} d_{km}^\beta \right) w_k. \quad (29)$$

The analytic expression of average trapping distance for Lévy walks We now study the trapping problem for Lévy walks at an arbitrarily given node. Let L_j be the average trapping distance, which is the mean of MFTD L_{ij} to the trap node j , taken over the stationary distribution defined as follows:

$$L_j = \frac{1}{1 - w_j} \sum_{i=1}^N w_i l_{ij}. \quad (30)$$

Substituting the expression of l_{ij} in Eq. (6) and w_j in Eq. (5) into Eq. (30) gives

$$L_j = \frac{1}{1 - w_j} \sum_{i=1}^N w_i \left(\frac{z_{jj} - z_{ij}}{w_j} \frac{\sum_i \sum_j d_{ij}^{\beta-\alpha}}{\sum_i \sum_j d_{ij}^{-\alpha}} \right) + \frac{1}{1 - w_j} \sum_{i=1}^N w_i \left(\sum_k (z_{ik} - z_{jk}) \left(\frac{\sum_m d_{km}^{\beta-\alpha}}{\sum_m d_{km}^{-\alpha}} \right) \right). \quad (31)$$

Using the fact that $wZ = w^{17}$ and with some calculation one obtains

$$L_j = \frac{1}{1 - w_j} \frac{z_{jj}}{w_j} \frac{\sum_i \sum_j d_{ij}^{\beta-\alpha}}{\sum_i \sum_j d_{ij}^{-\alpha}} + \frac{1}{1 - w_j} \sum_k z_{jk} \left(\frac{\sum_m d_{km}^{\beta-\alpha}}{\sum_m d_{km}^{-\alpha}} \right). \quad (32)$$

Empirically we find that the simulation values of the last term is far less than that of the first term and can be neglected in the analysis. In this context, Eq. (32) reduces to

$$L_j \approx \frac{z_{jj}}{K_j} \sum_i \sum_j d_{ij}^{\beta-\alpha}, \quad (33)$$

where $K_j = \sum_m d_{jm}^{-\alpha}$ named the long-range degree of node j ¹³. Here, we omit the value w_j as it can be approximated as zero when the network size N is very large. Moreover, for the fractal network with the fractal dimension d_f , the network diameter M can be approximated as $M \sim N^{\frac{1}{d_f}}$. Approximating M as a continuous variable, the term $\sum_i \sum_j d_{ij}^{\beta-\alpha}$ scales as²⁷

$$\sum_i \sum_j d_{ij}^{\beta-\alpha} \sim N \int_1^M x^{\beta-\alpha} x^{d_f-1} dx \sim \begin{cases} N \frac{N^{\frac{d_f+\beta-\alpha}{d_f}-1}}{\beta+d_f-\alpha}, & \alpha \neq d_f + \beta \\ \frac{N \ln N}{d_f}, & \alpha = d_f + \beta \end{cases}. \quad (34)$$

Plugging Eq. (34) into Eq. (33), we have a linear relationship between $\ln L_j$ and β (i.e., $\ln L_j \sim C\beta$ where C is a constant value determined by the fractal dimension d_f), when the position of the trapping node j and the tuning exponent α are fixed.

References

1. Barabási, A. L. The network takeover. *Nat. Phys.* **8**, 14–16 (2012).
2. Noh, J. D. & Rieger, H. Random walks on complex networks. *Phys. Rev. Lett.* **92**, 118701 (2004).
3. Condamin, S., Bénichou, O., Tejedor, V., Voituriez, R. & Klafter, J. First passage times in complex scale-invariant media. *Nature (London)* **450**, 77–80 (2007).
4. Hwang, S., Lee, D. S. & Kahng, B. First passage time for random walks in heterogeneous networks. *Phys. Rev. Lett.* **109**, 088701 (2012).
5. Perra, N. *et al.* Random walks and search in time-varying networks. *Phys. Rev. Lett.* **109**, 238701 (2012).
6. Lin, Y. & Zhang, Z. Z. Mean first-passage time for maximal-entropy random walks in complex network. *Sci. Rep.* **4**, 5365 (2014).
7. Yang, Z. M. & Zhou, T. Epidemic spreading in weighted networks: An edge-based mean-field solution. *Phys. Rev. E* **85**, 056106 (2012).
8. Skardal, P. S., Taylor, D. & Sun, J. Optimal synchronization of complex networks. *Phys. Rev. Lett.* **113**, 144101 (2014).
9. Li, G. *et al.* Towards design principles for optimal transport networks. *Phys. Rev. Lett.* **104**, 018701 (2010).
10. Patti, F. D., Fanelli, D. & Piazza, F. Optimal search strategies on complex multi-linked networks. *Sci. Rep.* **5**, 9869 (2015).
11. Viswanathan, G. M. Ecology: Fish in Lévy-flight foraging. *Nature (London)* **465**, 1018–1019 (2010).
12. Raichlen, D. *et al.* Evidence of Lévy walk foraging patterns in human hunter-gatherers. *Proc. Natl. Acad. Sci. U.S.A.* **111**, 728–733 (2014).
13. Riascos, A. P. & Mateos, J. L. Long-range navigation on complex networks using lévy random walks. *Phys. Rev. E* **86**, 056110 (2012).
14. Riascos, A. P. & Mateos, J. L. Fractional dynamics on networks: Emergence of anomalous diffusion and Lévy flights. *Phys. Rev. E* **90**, 032809 (2014).
15. Langville, A. N. & Meyer, C. D. *Google's PageRank and Beyond: The Science of Search Engine Rankings* (Princeton University, 2006).
16. Li, D. Q., Kosmas, K., Armin, B. & Shlomo, H. Dimension of spatially embedded networks. *Nat. Phys.* **7**, 481–484 (2011).
17. Grinstead, C. M. & Snell, J. L. *Introduction to Probability* (American Mathematical Society, 2006).
18. Kemeny, J. G. & Snell, J. L. *Finite Markov Chains* (van Nostrand Princeton, NJ, 1960).
19. Kozak, J. J. & Balakrishnan, V. Analytic expression for the mean time to absorption for a random walker on the Sierpiński gasket. *Phys. Rev. E* **65**, 021105 (2002).
20. Rozenfeld, H. D., Havlin, S. & ben-Avraham, D. Fractal and transfractal recursive scale-free nets. *New J. Phys.* **9**, 175 (2007).
21. Lin, Y. & Zhang, Z. Z. Random walks in weighted networks with a perfect trap: An application of Laplacian spectra. *Phys. Rev. E* **87**, 062140 (2013).
22. Barabási, A. & Albert, R. Emergence of scaling in random networks. *Science* **286**, 509–512 (1999).

23. Lusseau, D. *et al.* The bottlenose dolphin community of Doubtful Sound features a large proportion of long-lasting associations. *Behav. Ecol. Sociobiol.* **54**, 396–405 (2003).
24. Guimerà, R., Danon, L., Díaz-Guilera, A., Giralt, F. & Arenas, A. Self-similar community structure in a network of human interactions. *Phys. Rev. E* **68**, 065103 (2003).
25. Leskovec, J., Lang, K. J., Dasgupta, A. & Mahoney, M. W. Community structure in large networks: Natural cluster sizes and the absence of large well-defined clusters. *Internet Mathematics* **6**, 29–123 (2009).
26. Mcauley, J. & Leskovec, J. Learning to Discover Social Circles in Ego Networks. *Adv. Neural Inf. Process. Syst.* **25**, 548–556 (2012).
27. Li, G. *et al.* Optimal transport exponent in spatially embedding networks. *Phys. Rev. E* **87**, 042810 (2013).
28. Sommer, C. Shortest path queries in static networks. *ACM Computing Surveys* **46**, 45 (2014).

Acknowledgements

J.Z. is supported by National Science Foundation of China NSFC 61104143. We thank Kai Zhang for useful discussions and helps.

Author contributions statement

T. F. Weng, J. Zhang, M. Small and P. Hui designed the research, performed the research, and wrote the manuscript. K. Moein and R. Zheng analyzed data and performed research. All authors reviewed the manuscript.

Additional information

Competing financial interests: The authors declare no competing financial interests.